Supplementary Appendix

For

Identification of Enhanced Interferon-Gamma Signaling in Polyarticular Juvenile Idiopathic Arthritis with Mass Cytometry

Table of Contents

Supplemental Data

Case series of three refractory polyarticular JIA patients successfully treated with tofacitinib (a JAK inhibitor).....3-5

Supplementary Tables

Table S1: Surface and intracellular antibodies for CyTOF 6

Table S2: Antibody panels for flow cytometry 7

Table S3: Number of patient and control samples for each stimulation condition.....8

Table S4: Gating scheme for PBMC types from live immune cells 9

Supplementary Figures

Figure S1: Gating scheme for live singlet immune cells 10

Figure S2: Analysis of fresh and frozen PBMC signaling.....11

Figure S3: Analysis of preliminary polyarticular JIA patient sample via CyTOF done with 8 cytokines.....12

Figure S4: Citrus hierarchical clustering for IFNγ stimulated treatment-naïve patients versus controls 13

Figure S5: Citrus results for IFNγ stimulated treatment-naïve versus remission patients.....14

Figure S6: Citrus hierarchical clustering for IFNγ stimulated treatment-naïve versus remission patients.....15

Figure S7: SAM results for IFNγ stimulated treatment-naïve patients versus controls.....16

Figure S8: Median surface marker expression for stratifying and non-stratifying CD4 T cell clusters.....17

Figure S9: Median surface marker expression for stratifying and non-stratifying monocyte clusters.....18

Figure S10: Analysis of monocyte and naïve CD4 T cell IFNγ signaling cascade via flow cytometry.....19

Figure S11: Analyze of monocyte and CD4 T cell and subset proliferation.....20

Figure S12: p-STAT1 and p-STAT3 in RF+ and RF- patients……21
Figure S13: p-STAT1 and p-STAT3 with tofacitinib treatment……22

Case Series of three refractory polyarticular JIA patients successfully treated with tofacitinib (a JAK inhibitor)

Despite the efficacy of currently-available biologic therapies, polyarticular JIA remains difficult to control in a nontrivial subset of patients, underscoring the need for additional therapeutic approaches to the treatment of this disorder. The identification of enhanced responsiveness to IFNγ stimulation in subsets of CD4 T cells and classical monocytes from treatment-naïve polyarticular JIA patients highlights the possibility that specifically targeting the IFNγ signaling pathway with a Janus Kinase (JAK) inhibitor (e.g., tofacitinib) may be beneficial in polyarticular JIA.

Tofacitinib has been FDA approved for use in moderate to severe rheumatoid arthritis; however, we are not aware of any case reports or case series reporting the use of tofacitinib in polyarticular JIA patients other than a single case of its use in a 58 year old woman with a past history of polyarticular JIA and onset of refractory colitis in her thirties. Below, we present three refractory polyarticular JIA patients who had positive responses to treatment with tofacitinib at our medical center. All three were adolescent, RF+, Caucasian females who had failed to gain durable clinical remission with other biologic agents.

Case 1

A 7-year-old Caucasian female presented to an outside institution with a three month history of arthralgia and limitation in range of motion of her neck, ankles, knees, shoulders, and wrists. She was diagnosed with RF+ polyarticular JIA. Initial treatment by the outside provider included weekly intravenous steroid pulses and oral methotrexate (MTX), and she initially achieved prolonged clinical remission. Etanercept was added after a flare in her disease at age 12 but failed to induce a durable remission. She transferred her care to our institution at age 13 with active arthritis affecting her wrists, elbows, hips, knee, and ankles. Laboratory evaluation at that time showed microcytic anemia (Hgb 9.9 g/dl; MCV 74.4) and elevated inflammatory markers (ESR 106 mm/hr, CRP 54 mg/L). Serologic testing revealed a positive anti-nuclear antibody (ANA) (1:320), rheumatoid factor (296 units/ml), and anti-CCP (>250 units).

Her etanercept was replaced by adalimumab, and her MTX was converted to subcutaneous dosing with concomitant intra-articular steroid injections of multiple active joints. After six months she had not achieved clinical remission, so adalimumab was stopped, and she was given a course of rituximab with symptomatic improvement. When her disease flared after five months with bilateral wrist arthritis, she was given a second course of rituximab (requiring four doses due to incomplete CD19 depletion) and continued on MTX. She again had a good but not durable response to rituximbab. Within 9 months, she developed new-onset shoulder involvement and recurrence of arthritis in her fingers, wrists, elbows, hips, and ankles with numerous contractures. Golimumab and hydroxychloroquine were added with an initial good response, but after six months, she had worsening hand symptoms with new erosions in her proximal interphalangeal (PIP) and metacarpeal (MCP) joints documented by x-ray. Golimumab was replaced by weekly subcutaneous tocilizumab with modest improvement, and she subsequently developed severe erosive disease in her left shoulder that did not improve with intra-articular steroid injection. Tocilizumab was then replaced with abatacept, which after three months demonstrated no improvement in controlling her disease particularly of her left shoulder, which was severely limiting her activities of daily living.

Therefore, abatacept was stopped and tofacitinib was started when she was 16 years old. She was also continued on hydroxychloroquine and leflunomide. After two months she had significant improvement with near resolution of her morning stiffness and increased range of motion in her left

shoulder, although she still had a number of swollen joints. Therefore, low-dose sulfasalazine was added, and her hydroxychloroquine was stopped. After six months of tofacitinib, her left shoulder had regained approximately 80% of its normal range of motion with resolution of associated pain or stiffness, and she had only a single active joint (a PIP) that subsequently resolved over the next several months. Nearly one year after starting tofacitinib, she remains in clinical remission and is tolerating the tofacitinib in combination with leflunomide and sulfasalazine.

Case 2

A 16-year-old Caucasian female presented with two years of progressively worsening and additive arthralgia/arthritis. At presentation, she had involvement of her right knee, bilateral wrists, and multiple PIP and MCP joints as well as bilateral 1st-4th metatarsophalangeals (MTP), tibiotalar, subtalar and talonavicular synovitis and associated tenosynovitis (confirmed by MRI). Other features included livedo reticularis and Raynaud's phenomenon. Laboratory evaluation at presentation revealed normocytic anemia (Hgb 11 g/dl; MCV 87.8) and elevated inflammatory markers (ESR 57 mm/hr; CRP 24.7 mg/L) with normal C3 and C4 complement levels. Serologic testing showed strongly positive rheumatoid factor (98 units/ml) and anti-CCP (>250 units) with negative ANA, extractable nuclear antibodies (ENA), anti-double stranded DNA antibodies, and antiphospholipid antibodies.

She was diagnosed with RF+ polyarticular JIA, and her initial treatment consisted of oral prednisone and subcutaneous methotrexate. She had improvement with prednisone, but repeatedly worsened as it was weaned. After 2 months, etanercept was added. Her symptoms did not improve, and after a three month trial, etanercept was replaced by adalimumab with the addition of hydroxychloroquine. She had some symptomic improvement over a three-month period, but a repeat MRI demonstrated erosive synovitis and tenosynovitis in her right hand and wrist. Adalimumab was replaced by weekly subcutaneous tocilizumab. However, after three months, her symptoms had not improved, and an MRI showed progressive disease involving her right hand and wrist. Tocilizumab was then stopped, and she was given a course of rituximab with complete CD19 depletion but only partial improvement of symptoms. Abatacept was added several months later, and methotrexate was replaced with leflunomide for a period of six months with minimal improvement and continued MRI evidence of active synovitis in her right hand and wrist.

At that point, abatacept was replaced with tofacitinib. Over a three-month period, she showed improvement in pain, morning stiffness, and function. Repeat MRI of her hands after six months of therapy with tofacitinb showed resolved synovitis, no new erosions, and improved tenosynovitis. She has now been maintained on tofacitinib in combination with leflunomide and hydroxychloroquine for 9 months without any adverse effects such as cytopenias, abnormal chemistries, or recurrent infections.

Case 3

A 14-year-old Caucasian female presented with two years of arthralgia and joint swelling (including hands, elbows, shoulders, hips, knees and feet). She was initially diagnosed with RF+ polyarticularly JIA at another institution and prescribed methotrexate. She did not start the methotrexate and was lost to follow-up for 11 months until she presented to our clinic. Physical exam showed synovitis in her bilateral 1st-3rd MCPs, and MRI demonstrated synovitis and joint effusions involving her right shoulder and left hip. Laboratory evaluation showed normal blood counts and negative inflammatory markers. Serologic testing showed positive ANA (1:160), rheumatoid factor (65 units/ml), and anti-CCP (>250 units).

Initial treatment including weekly oral methotrexate and etanercept induced sustained remission over a 12-month period. However, withdrawal of etanercept resulted in rapid recrudescence of active

arthritis. Indeed, she experienced flares repeatedly when her injections were late or missed. Her methotrexate was switched to leflunomide to minimize the number of injections and improve compliance. However, difficulty in consistency with weekly injections resulting in frequent disease recurrences lead us to change her therapy to tofacitinib and leflunomide as she was transitioning to college. She has currently been using tofacitinib in combination with leflunomide for over five months with sustained remission and no adverse effects.

Table S1. Surface and intracellular antibodies for CyTOF.

Antigen Target (Human)	Clone Number	Supplier	Elemental isotope	Dilution (from recommended)
CD45	HI30	Fluidigm	89Y	0.3X
CD19	HIB19	Fluidigm	142Nd	0.33x
CD45RA	HI100	Fluidigm	143Nd	0.1x
CD4	RPA-T4	Fluidigm	145Nd	0.33x
CD8a	RPA-T8	Fluidigm	146Nd	1x
CD7	CD7-6B7	Fluidigm	147Sm	0.33x
CD16	3G8	Fluidigm	148Nd	1x
CD66	CD66a-B1.1	Fluidigm	149Sm	0.33x
CD123 (IL3r)	6H6	Fluidigm	151Eu	0.33x
CD163	GHI/61	Fluidigm	154Sm	1X
CD27	L128	Fluidigm	155Gd	0.1x
CD11c	Bu15	Fluidigm	159Tb	0.33x
CD14	M5E2	Fluidigm	160Gd	1x
CD69	FN50	Biolegend	163Dy	0.5ug/ml
CD45RO	UCHL1	Fluidigm	165Ho	0.33x
CD25 (IL2Rα)	2A3	Fluidigm	169Tm	1x
CD3	UCHT1	Fluidigm	170Er	0.33x
CD38	HIT2	Fluidigm	172Yb	1x
HLADR	L243	Fluidigm	173Yb	0.1X
CD56	NCAM16.2	Fluidigm	176Yb	0.03x
CD11b	ICRF44	Fluidigm	209Bi	1x
pSHP2	D66F10	Fluidigm	141Pr	1x
p-PLCγ2	K86-698.37	Fluidigm	144Nd	0.33
p-STAT5	47	Fluidigm	150Nd	1x
p-AKT	D9E	Fluidigm	152Sm	1x
p-STAT1	58D6	Fluidigm	153Eu	1x
p-p38	D3F9	Fluidigm	156Gd	1x
p-STAT3	4/P-Stat3	Fluidigm	158Gd	1x
Ki-67	B56	Fluidigm	161Dy	1x
p-LCK	K86-689.37	Fluidigm	162Dy	0.1x
IκB	L35A5	Fluidigm	164Dy	1x
p-p65-NFkB	K10-895	Fluidigm	166 Er	0.1x
p-ERK1/2	D13.14.4E	Fluidigm	167Er	1x
p-STAT6	18	Fluidigm	168Er	0.33x
p-ZAP70/p-Syk	17a	Fluidigm	171Yb	1x
pSTAT4	38	Fluidigm	174Yb	0.33x
pS6	N7-548	Fluidigm	175Lu	0.3x

Table S2. Antibody panels for flow cytometry.

Antigen Target (Human)	Clone Number	Supplier	Fluorophore	Catalog Number	Final Concentration	Monocyte Panel 1	Monocyte Panel 2	CD4 T cell Panel 1	CD4 T cell Panel 2
SOCS1	Polyclonal	Abcam	FITC	ab9870	19.2ng/ml	X		X	
PIAS1	D33A7	CST	PE	#92725	0.65ng/ml	X		X	
p-STAT3	4/P-STAT3	BD	PerCP-Cy5.5	560114	1:5	X		X	
CD45RO	UCHL1	Biolegend	PE-Cy7	304230	10µg/ml	X	X	X	X
p-STAT1	58D6	CST	AF647	#8009s	0.5µg/ml	X		X	
CD14	M5E2	Biolegend	Pac Blue	301828	20µg/ml	X	X		
CD16	3G8	BD	V500	561394	1:20	X	X		
HLA-DR	G46-6	BD	BV786	564041	1:20	X	X		
CD3	UCHT1	BD	BV395	563546	1:20			X	X
IFNGR1	GIR-208	Biolegend	PE	308606	10µg/ml		X		X
JAK2	Polyclonal	Assaypro	PerCP	33028-05171	37.5µg/ml		X		X
JAK1	REA700	Miltenyi	APC	130-110-550	1:50		X		X
CD4	RPA-T4	Biolegend	APC/Fire750	317415	10µg/ml			X	X
CD45RA	HI100	Biolegend	Pac Blue	304123	10µg/ml			X	X
CD38	HIT2	Biolegend	BV510	303540	7.5µg/ml			X	X
CD27	L128	BD	BV786	563327	1:20			X	X
CD14	M5E2	Biolegend	APC/Fire750	301854	20µg/ml				
CD4	RPA-T4	BD	PE	55347	1:5				

Table S3. Number of patient and control samples for each stimulation condition.

Of note, one of the 17 treatment-naïve patients (Pt 4) was used in preliminary experiments (including Figure S3) and not included in the primary analyses.

	Treatment-naïve Patients	Remission Patients	Controls
Unstimulated	16	10	19
IL-6 Stimulated	11	6	15
IFNγ Stimulated	15	11	19

Table S4. Gating scheme for PBMC types from live immune cells.

Cell Type	CD3	CD19	CD56	CD66a	CD123	CD14	HLA-DR	CD27	CD16	CD4	CD8	CD45RO	CD45RA	CD38	CD11c
Granulocytes	neg	neg		pos		neg									neg
Basophils	neg	neg		neg	pos	neg	neg							pos	neg
NK cells	neg	neg	pos		neg	neg									
Dim NK cells	neg	neg	low		neg	neg			high						
Bright NK cells	neg	neg	high		neg	neg			low						
NK T cells	pos	neg	pos		neg	neg									
Effector CD8 T cells	pos	neg			neg	neg	neg	neg		neg	pos		pos		
Activated CD8 T cells	pos	neg			neg	neg	pos			neg	pos			pos	
Memory CD8 T cells	pos	neg			neg	neg	neg	pos		neg	pos	pos	neg		
Naïve CD8 T cells	pos	neg			neg	neg	neg	pos		neg	pos	neg	pos		
Effector CD4 T cells	pos	neg			neg	neg	neg	neg		pos	neg		pos		
Activated CD4 T cells	pos	neg			neg	neg	pos			pos	neg			pos	
Memory CD4 T cells	pos	neg			neg	neg	neg	pos		pos	neg	pos	neg		
Naïve CD4 T cells	pos	neg			neg	neg	neg	pos		pos	neg	neg	pos		
Memory B cells	neg	pos			neg	neg	pos	pos							
Naïve B cells	neg	pos			neg	neg	pos	neg							
Plasma B cells	neg	pos			neg	neg	neg							pos	
B cells	neg	pos			neg	neg									
pDCs	neg	neg		neg	pos	neg	pos							pos	neg
mDCs	neg	neg			neg	neg	pos							pos	pos
Non-classical monocytes	neg	neg	neg		neg	neg	pos		pos						
Classical monocytes	neg	neg	neg		neg	pos	pos		neg						
Intermediate monocytes	neg	neg	neg		neg	pos	pos		pos						

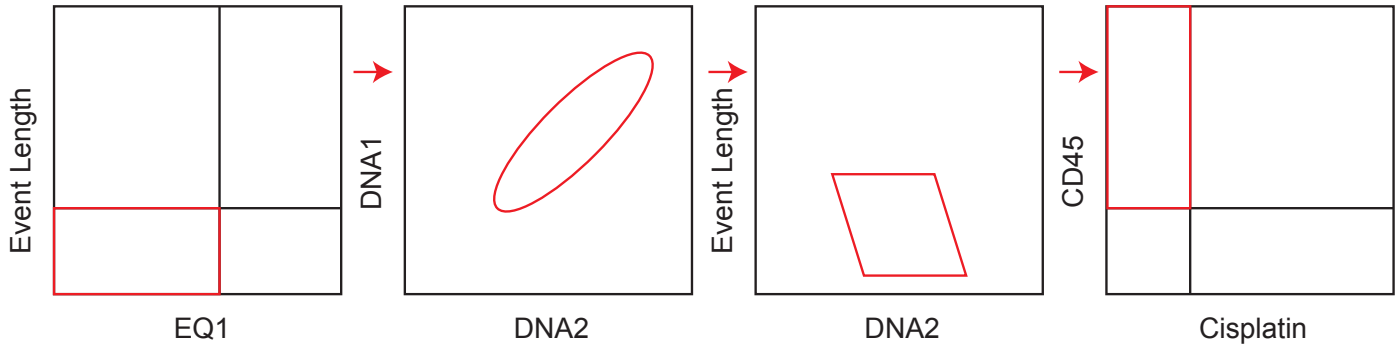

Figure S1. Gating scheme for live singlet immune cells.

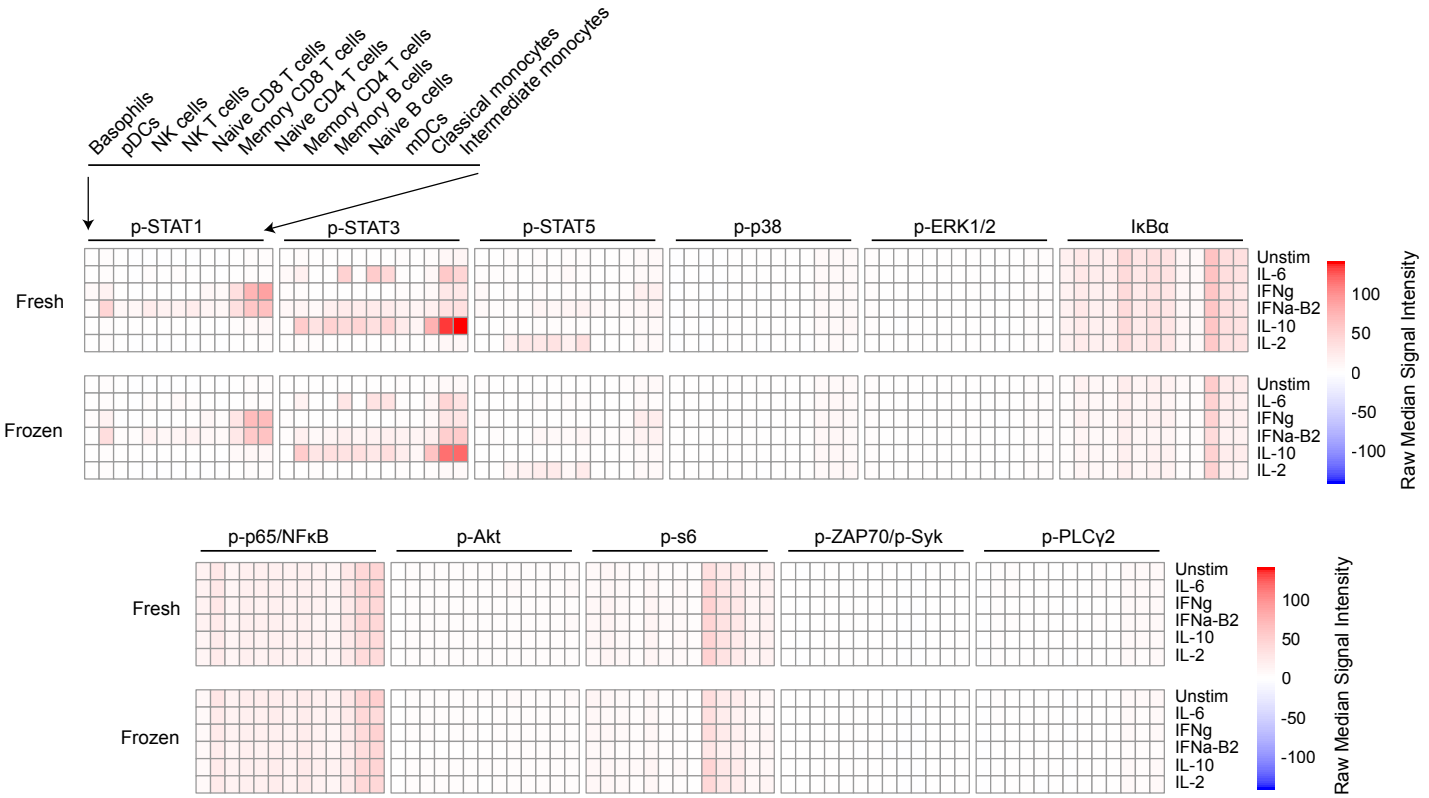

Figure S2. There is no difference in phosphorylation of signaling molecules in 13 cell types following 5 different stimulations between cell types of fresh and frozen samples collected from a single donor. Samples were stimulated 30 minutes with specified cytokines. Heat map of raw signaling molecule median intensity in different peripheral blood mononuclear cells (PBMCs) in response to different stimulations in fresh and frozen samples in shown cell populations. Columns for each signaling molecule correspond to the following cell types: basophils, pDCs, NK cells, NK T cells, naïve CD8 T cells, memory CD8 T cells, naïve CD4 T cells, memory CD4 T cells, memory B cells, naïve B cells, mDCs, classical monocytes, intermediate monocytes.

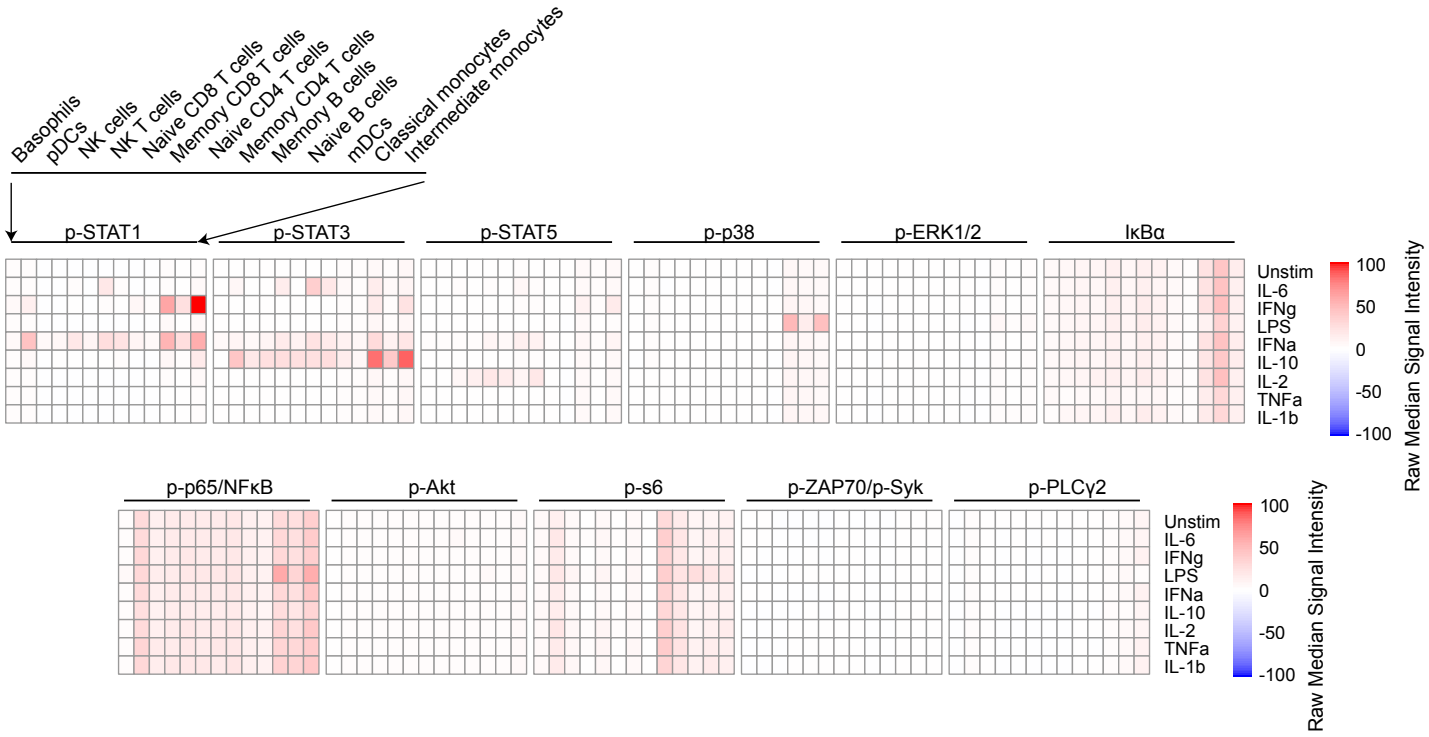

Figure S3. Analysis of a preliminary polyarticular juvenile idiopathic arthritis (JIA) patient sample via CyTOF done with broad array of 8 cytokines. Samples were stimulated 30 minutes with specified cytokines. Heat map of raw signaling molecule median intensity in different cell types in response to different stimulations. Columns for each signaling molecule correspond to the following cell types: basophils, pDCs, NK cells, NK T cells, naïve CD8 T cells, memory CD8 T cells, naïve CD4 T cells, memory CD4 T cells, memory B cells, naïve B cells, mDCs, classical monocytes, intermediate monocytes.

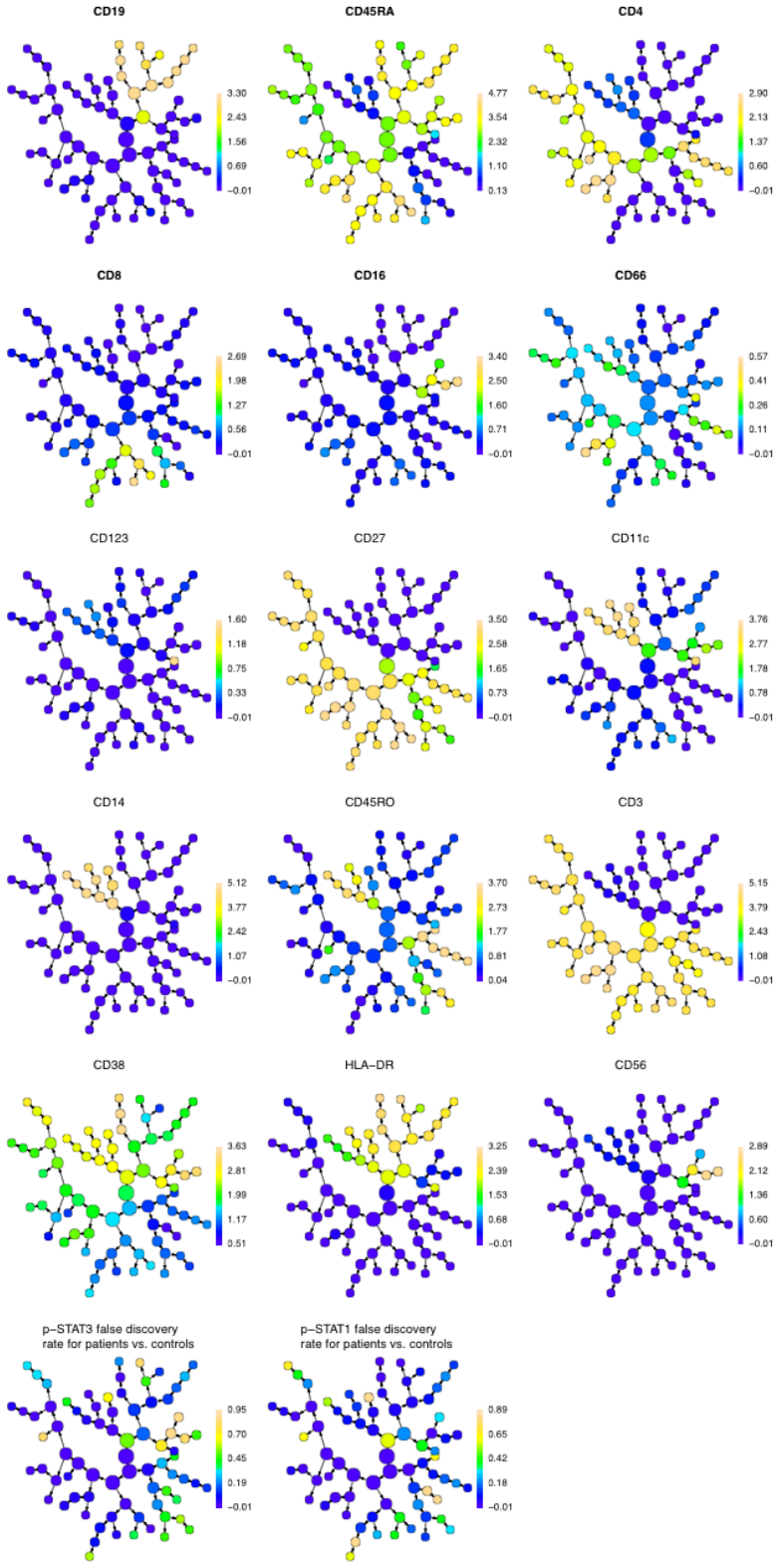

Figure S4. Citrus hierarchical clustering for IFNγ stimulated treatment-naïve patients (n=15; Pt4 and Pt5 were excluded due to lack of treatment-naïve IFNγ stimulated sample) versus controls (n=19) colored by arcsinh transform of median marker intensity, p-STAT1 and p-STAT3 false discovery rate comparing treatment naïve patient and control samples for each cluster for the bottom two plots. False discovery rate is an empirically calculated approximation for a p-value for the respective signaling molecules computed by permuting patient and control labels. Arrows indicate a child/children emanating from a parent cluster.

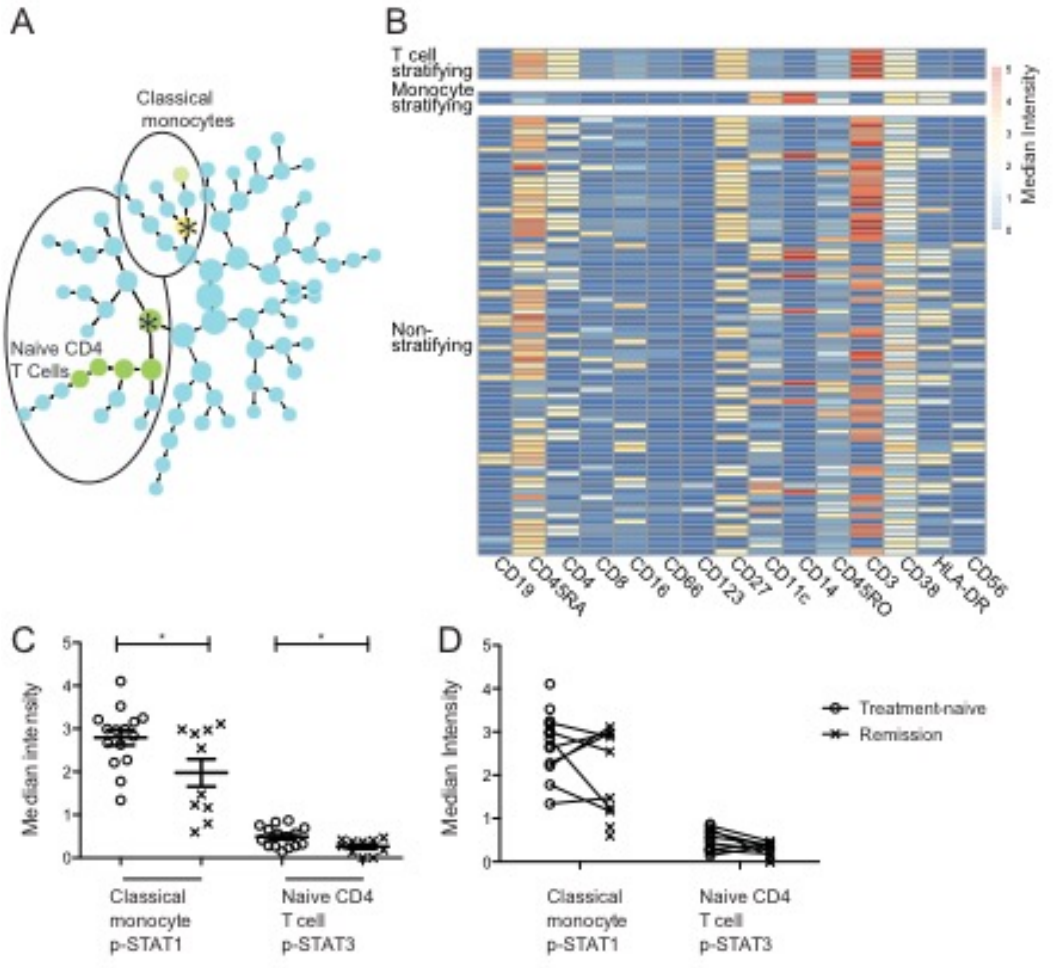

Figure S5. Classical monocyte subsets more strongly phosphorylate STAT1 in 16 treatment-naïve patients than a subset of 10 of the 16 patients in remission with IFNγ stimulation, while CD4 T cells subsets have greater levels of STAT3 phosphorylation in treatment-naïve patients than remission patients after IFNγ stimulation. N=15 treatment naïve patients, N=10 remission patients. Pt4 and Pt5 were excluded due to lack of treatment-naïve IFNγ stimulated sample. A) Hierarchical clustering for IFNγ stimulated treatment-naïve patient versus remission patient PBMCs. Non-stratifying clusters are light blue for q<0.05, p-STAT3 stratifying (different between patients and controls for a signaling molecule) clusters are green, p-STAT1 stratifying clusters are yellow, B) Heat map depicting surface marker intensities for stratifying and non-stratifying classical monocyte and CD4 T cell clusters, C) Arcsinh transformed median phosphoprotein intensities for largest stratifying CD4 T cell and classical monocyte clusters denoted with asterisks (classical monocyte p-STAT1: t=2.416, df=23, p=0.0240; CD4 T cell p-STAT4: t=2.635, df=23, p=0.0148). Open circles denote treatment naïve patients and X's denote remission patients, D) Arcsinh transformed median phosphoprotein intensities for largest stratifying CD4 T cell and classical monocyte clusters denoted with asterisks with paired treatment-naïve and remission patient samples. p-STAT1 (one-tailed paired t-test: t=0.394, df=7, p=0.705) in largest stratifying classical monocyte cluster and p-STAT3 (one-tailed paired t-test: t=1.718, df=7, p=0.130) in largest stratifying naïve CD4 T cell cluster with cessation of active disease (from IFNγ stimulated treatment-naïve versus remission patient Citrus) between paired treatment-naïve patient and remission patient IFNγ stimulated samples (n=8 paired treatment-naïve and remission patient samples; n=15 treatment-naïve patients and n=10 remission patients; Pt 4 and Pt 5 were excluded, as they did not have IFNγ stimulated samples). Median intensity of p-STAT1 and p-STAT3 is visualized as the arcsinh transform of the raw median intensity.

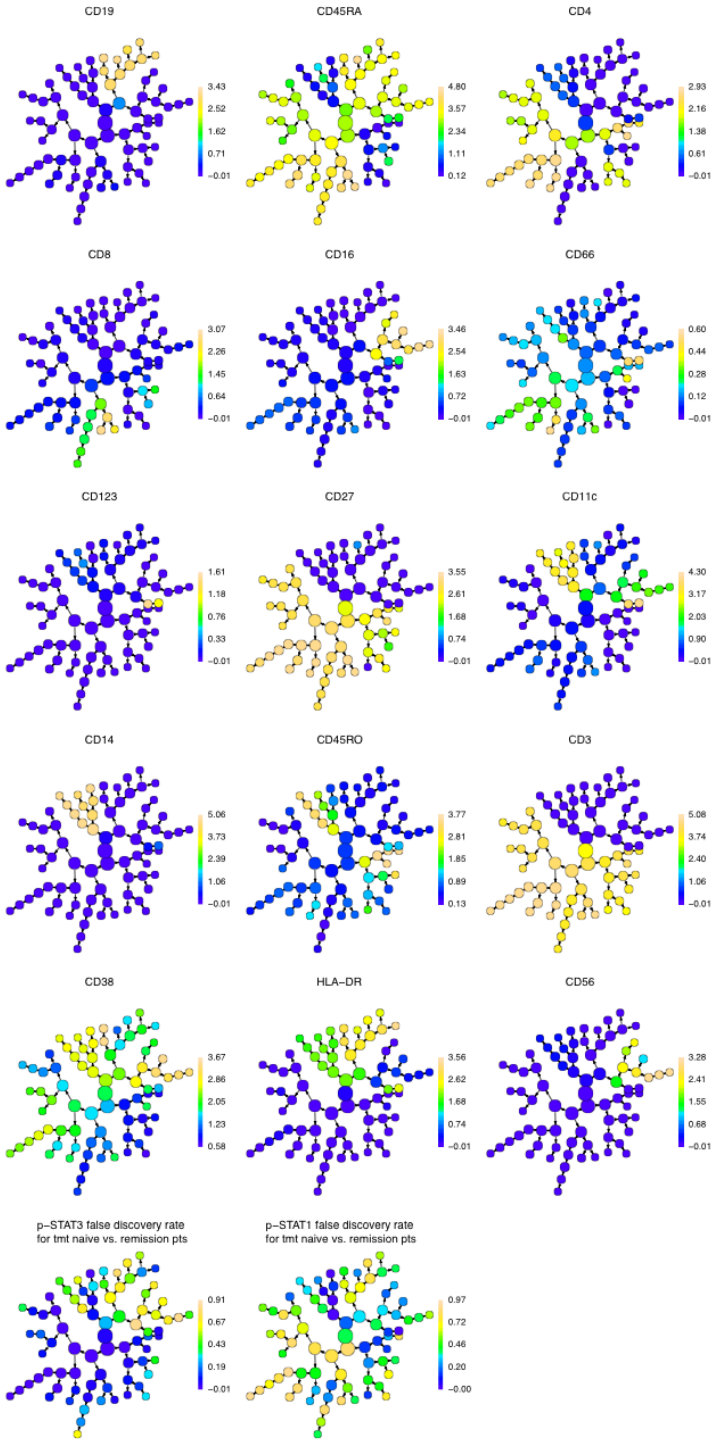

Figure S6. Citrus hierarchical clustering for IFNγ stimulated treatment-naïve patients (n=15) versus remission patients (n=10) colored by arcsinh transform of median marker intensity, p-STAT1 and p-STAT3 false discovery rate comparing treatment naïve patient and remission patient samples for each cluster for the bottom two plots. Pt4 and Pt5 were excluded due to lack of IFNγ stimulated sample. Arrows indicate a child/children emanating from a parent cluster. See Figure S5 for explanation of false discovery rate.

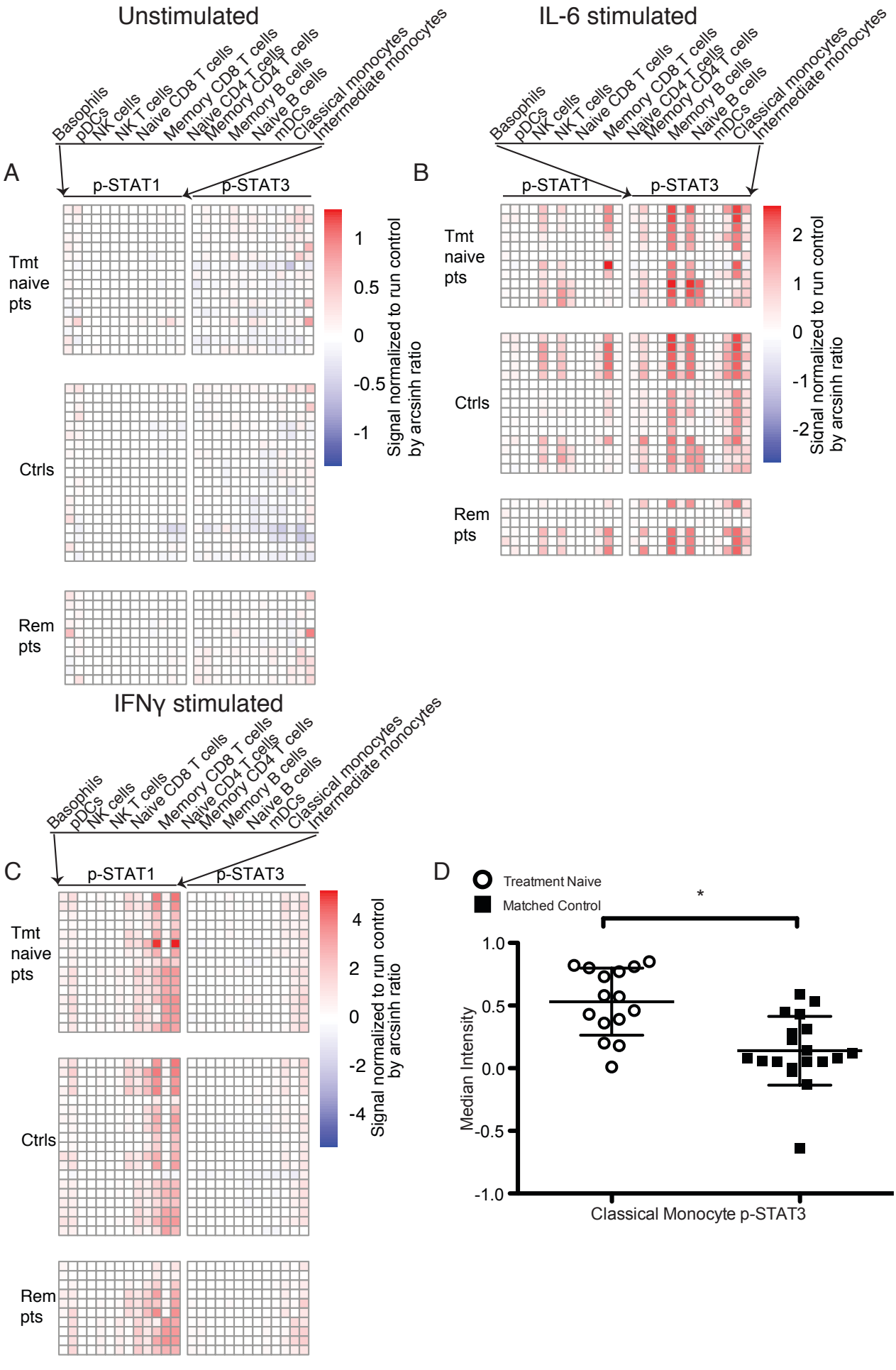
Unstimulated
IL-6 stimulated
IFNγ stimulated
Basophils
pDCs
NK cells
NK T cells
Naive CD8 T cells
Memory CD8 T cells
Naive CD4 T cells
Memory CD4 T cells
Memory B cells
Naive B cells
mDCs
Classical monocytes
Intermediate monocytes
A
B
C
p-STAT1
p-STAT3
Tmt naive pts
Ctrls
Rem pts
Signal normalized to run control by arcsinh ratio
1
0.5
0
-0.5
-1
2
-2
4
-4
D
Treatment Naive
Matched Control
*
Median Intensity
1.0
0.5
0.0
-0.5
-1.0
Classical Monocyte p-STAT3

Figure S7. There are no signaling differences between treatment-naïve patient and matched control PBMC signaling at baseline or with IL-6 stimulation as assessed by significance analysis of microarrays (SAM), but there are statistically significant signaling differences in p-STAT3 with IFNγ stimulation. Columns in the heat maps correspond to different cell types: basophils, pDCs, NK cells, NK T cells, naïve CD8 T cells, memory CD8 T cells, naïve CD4 T cells, memory CD4 T cells, memory B cells, naïve B cells, mDCs, classical monocytes, and intermediate monocytes. Color in heat maps represents intensity of p-STAT1 and p-STAT3 in these cell types for each specimen normalized to a run control using an arcsinh ratio. Patients and controls were excluded from certain stimulations due to low cell counts from these patients. A) Unstimulated signaling heat map (n=16 treatment-naïve patients, n=19 controls, n=10remission patients), B) IL-6 stimulated signaling heat map (n=10 treatment-naïve patients, n=15 controls, n=6 remission patients), C) IFNγ stimulated signaling heat map, D) Significant signaling differences between IFNγ stimulated treatment-naïve patient and control cells (classical monocyte p-STAT3: delta=4.18, q=0.030, two-tailed Student's t-test: t=4.17, df=32, p=0.0002; n=15 treatment-naïve patients, n=19 controls, n=10 remission patients).

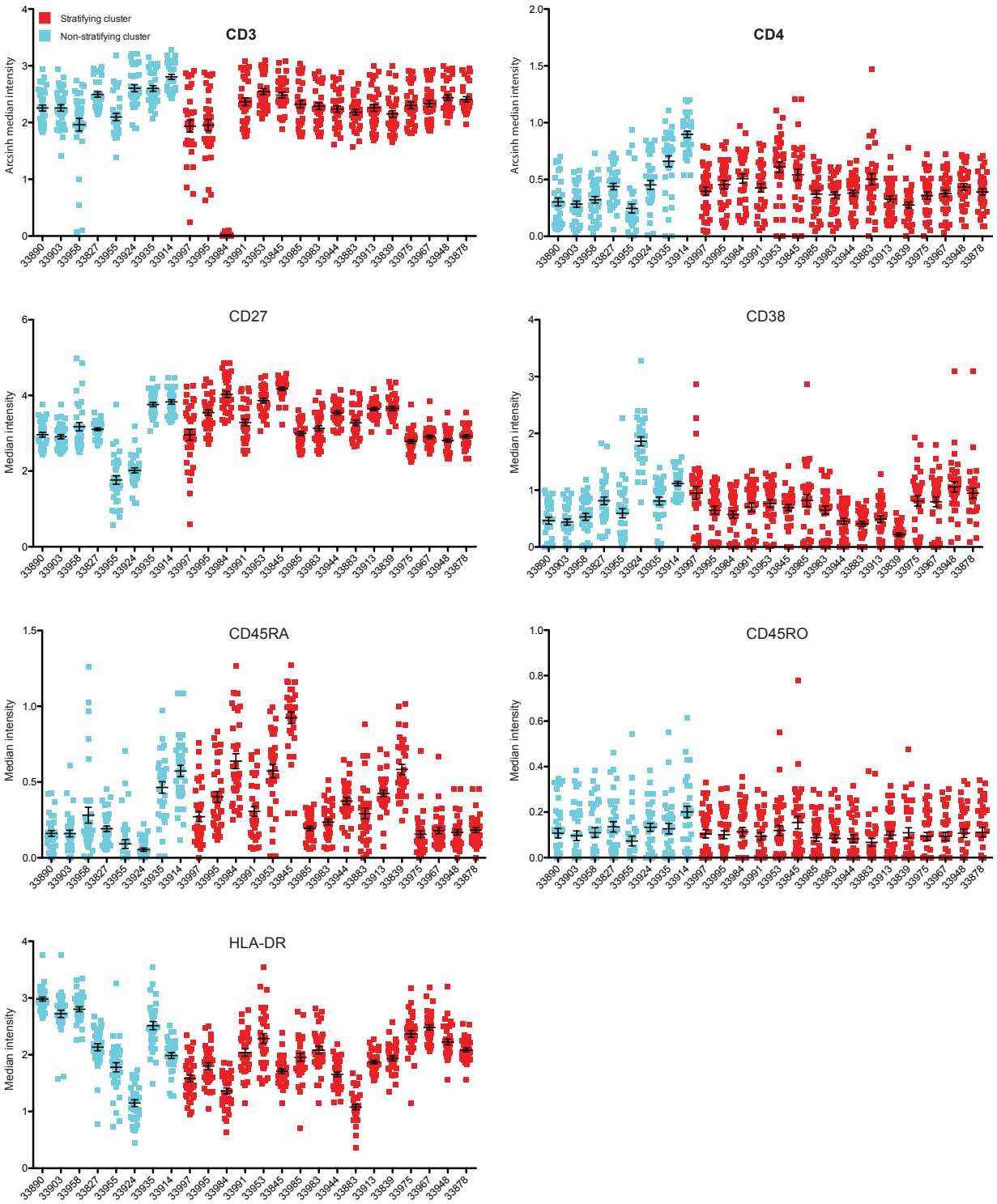

Figure S8. Arcsinh transformed median surface marker expression for all samples for stratifying (red) and non-stratifying (blue) naïve CD4 T cell clusters detected in Citrus comparing treatment naïve patient and controls with IFNγ stimulation for markers relevant to CD4 T cells (n=15 treatment-naïve patients and n=19 controls; Pt4 and Pt5 were excluded due to lack of IFNγ stimulated sample). See Figure 3 for location of specific clusters in hierarchical clustering tree. Non-stratifying clusters are listed from the distal to proximal parts of the tree and stratifying from proximal to distal.

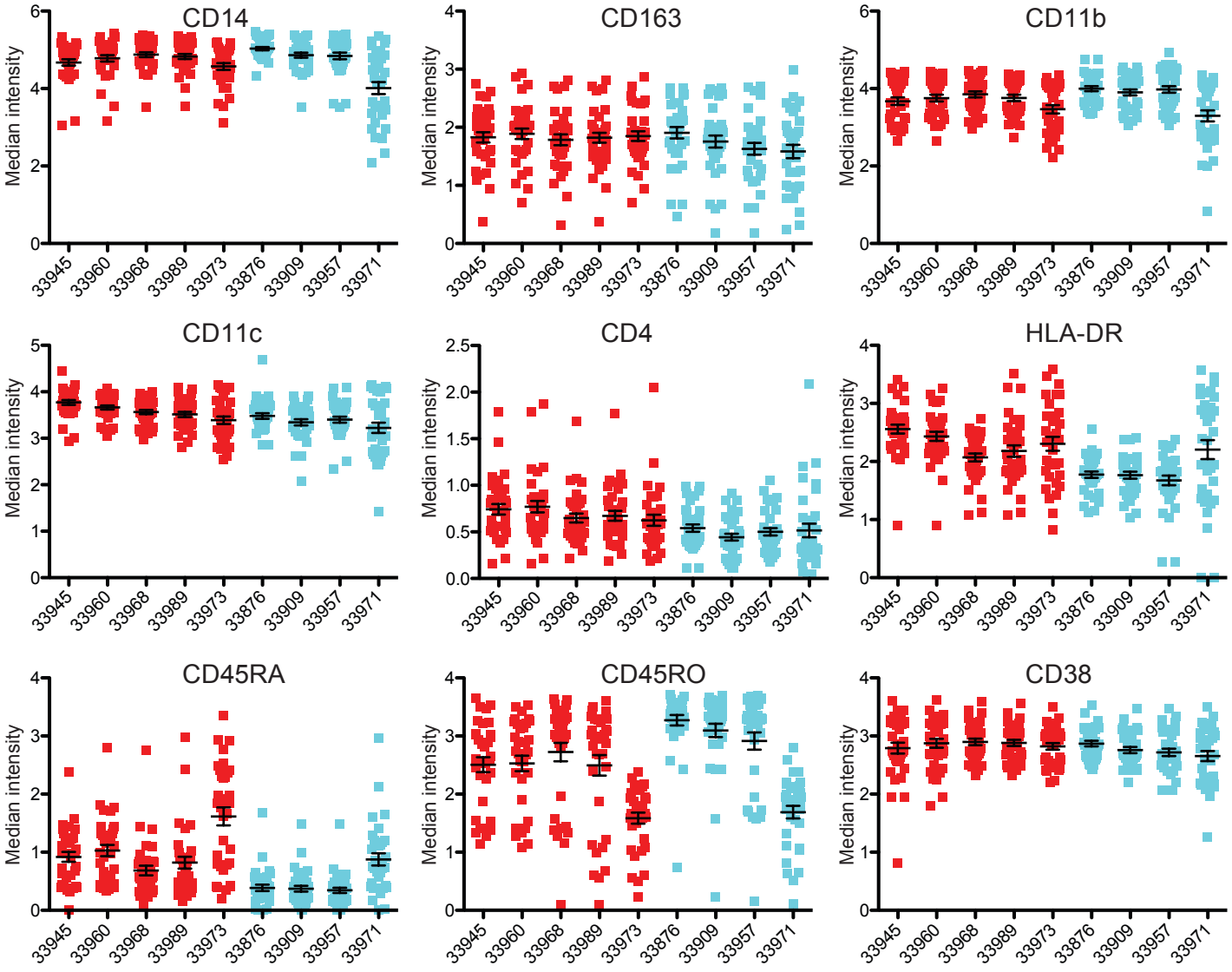

Figure S9. Arcsinh transformed median surface marker expression for all samples for stratifying (red) and non-stratifying (blue) classical monocyte clusters detected in Citrus comparing treatment naïve patient and controls with IFNγ stimulation for markers relevant to classical monocytes (n=15 treatment-naïve patients and n=19 controls; Pt4 and Pt5 were excluded due to lack of IFNγ stimulated sample). See Figure 4 for location of specific clusters in hierarchical clustering tree. Stratifying/non-stratifying nodes are listed from distal nodes on the left side monocyte branch to proximal to distal on the right side monocyte branch.

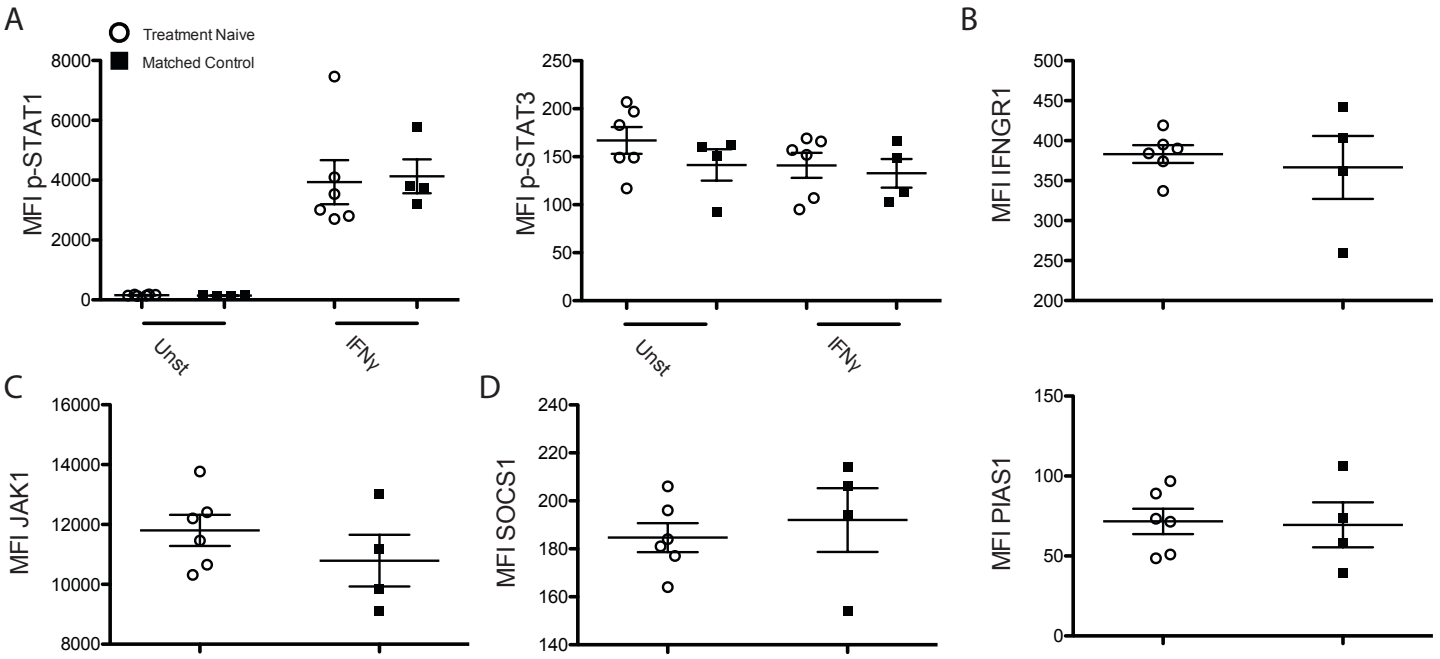

Figure S10. No signaling differences in IFNγ signaling cascade between treatment-naïve patients and controls in classical monocytes. N=6 treatment naïve patients and 4 controls. Not all patients had remaining samples and therefore were not included in flow cytometry analysis. A) STAT1 phosphorylation in patient and control classical monocytes with and without 250ng/ml IFNγ stimulation for 15 minutes (left panel; unstimulated: 2 tailed t=1.32, df=8, p=0.22; stimulated: t=0.19, df=8, p=0.85) and STAT3 (right panel; unstimulated: t=1.17, df=8, p=0.28; stimulated: t=0.41, df=8, p=0.69), B) JAK1 in unstimulated patient and control classical monocytes (t=1.08, df=8, p=0.31), C) Interferon Gamma Receptor 1 (IFNGR1) in unstimulated patient and control classical monocytes (t=0.489, df=8, p=0.64), D) Inhibitory molecules SOCS1 (left) and Protein Inhibitor of Activated STAT 1 (PIAS1) (right) in unstimulated patient and control classical monocytes (SOCS1: t=0.57, df=8, p=0.59, PIAS1: t=0.15, df=8, p=0.89).

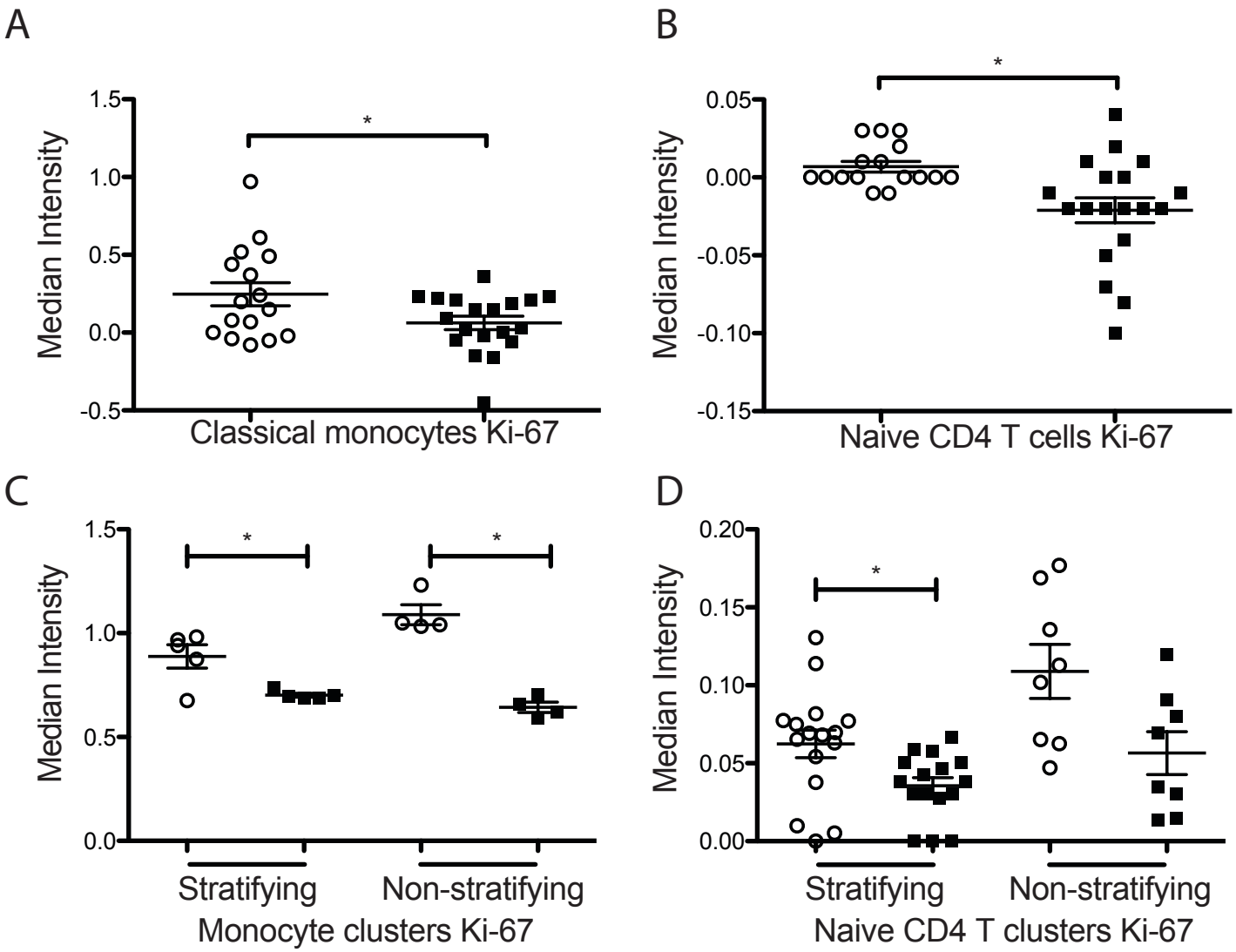

Figure S11. Signaling differences between treatment-naïve patients and controls in naïve CD4 T cells and classical monocytes correspond to higher levels of proliferation in manually gated populations and in populations clustered by Citrus. Open circles denote treatment naïve patients (n=16: Pt4 used in preliminary analyses was not analyzed using the same panel) and filled squares controls (n=19). A) Classical monocytes and B) naïve CD4 T cells are more actively proliferating in treatment-naïve patients than in controls, as suggested by levels of Ki-67. Ki-67 expression in classical monocytes ($t=2.14$, $df=24$, $p=0.043$) and naïve CD4 T cells ($t=3.22$, $df=24$, $p=0.004$), C) Ki-67 median intensity in stratifying and non-stratifying classical monocyte clusters detected by Citrus compared between patients and controls (stratifying: $t=3.28$, $df=8$, $p=0.011$; non-stratifying: $t=8.30$, $df=6$, $p=0.0002$), D) Ki-67 median intensity in stratifying and non-stratifying naïve CD4 T cell clusters detected by Citrus compared between patients and controls (stratifying: $t=2.61$, $df=30$, $p=0.014$; non-stratifying: $t=2.36$, $df=14$, $p=0.033$).

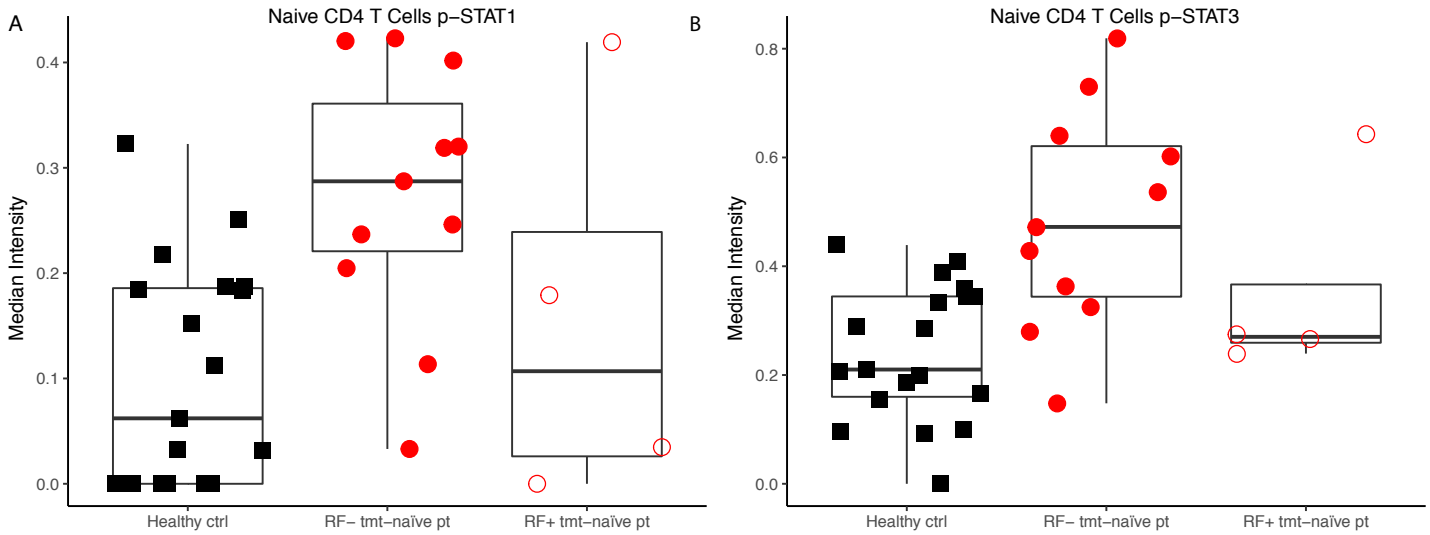

Figure S12. There is not statistical difference in naïve CD4 T cell IFNγ responsiveness between rheumatoid factor (RF) positive and negative patients (n=19 healthy controls, n=11 RF- treatment-naïve patients, n=4 RF+ treatment-naïve patients; RF+ patients 4 and 5 were excluded because Pt4 was used for preliminary analyses, and Pt5 did not have IFNγ stimulated samples). Data for the largest stratifying naïve CD4 T cell cluster (33995) visualized as the arcsinh median intensity was analyzed between treatment-naïve patients that were RF+ and RF-. A) p-STAT1 (two-tailed paired t-test: t=-1.12, df=3.98, p=0.325), B) p-STAT3 (two-tailed paired t-test: t=-1.14, df=5.65, p=0.299).

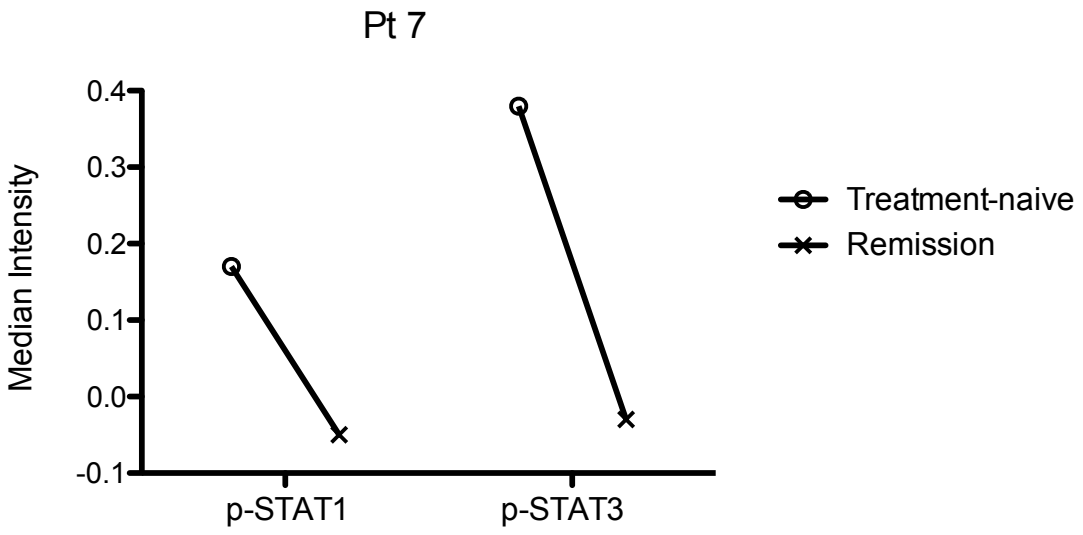

Figure S13. P-STAT1 and p-STAT3 phosphorylation are decreased in single paired treatment-naïve and remission patient treatment with tofacitinib (Pt 7 in Table1). A single patient (case 2) discussed in the Case Studies had a treatment-naïve sample included in the study (who had not achieved clinical remission before the initial CyTOF analysis was performed). A remission sample for the patient during tofacitinib treatment was obtained at a later date and analyzed via mass cytometry with IFNγ stimulation along with the same matched control. The samples were gated on naïve CD4 T cells and assessed for p-STAT1 and p-STAT3. Data are displayed are normalized as the arcsinh ratio of the patient sample to the same matched control.